2.10 THE INTERDECADAL VARIABILITY OF NORTHERN HEMISPHERE BLOCKING

David Barriopedro[1] Ricardo Garcia – Herrera[1] Anthony R. Lupo[2*] Emiliano Hernandez[1]

[1]Departmento de Fisica de la Tierra II
Facultad de Ciencias Fisicas
Universidad Complutense de Madrid, Cuidad Universitaria
Madrid, Spain 28040

[2]Department of Soil, Environmental, and Atmospheric Science
302 Anheuser Busch Natural Resources Building
University of Missouri-Columbia
Columbia, MO 65211

1. INTRODUCTION

During the middle of the previous century, most studies have defined blocking subjectively based on surface and/or mid-tropospheric observations of typical flow configurations. Following the traditional Rex (1950a) criterion, a blocking event can be identified by a split-flow regime in the middle troposphere as a double-jet detectable over more than 45º in longitude and persisting for more than 10 days. Since then, there have been several modifications to the original Rex definition, requiring smaller durations or extensions (Treidl et al., 1981) as well as restrictions in latitude location (White and Clark, 1975) in order to exclude semi-permanent subtropical anticyclones.

More recently, numerous criteria have been proposed in order to identify objectively atmospheric blocked flows. Most of them are based on zonal flow indices computed from meridional height gradients at the middle troposphere (Lejenäs and Økland, 1983 (*henceforth LO83*); Tibaldi and Molteni, 1990 (*henceforth TM90*); Trigo et al., 2004). Other methodologies detect blocking events as positive height anomalies in the mid-troposheric flow persisting for several days (e.g., Dole and Gordon, 1983) or from normalized indexes based on daily height projections over mean blocking patterns (Liu, 1994; Renwick and Wallace, 1996). The most recent methods combine traditional subjective and objective criteria, as those used by Lupo and Smith (1995) (*henceforth LS95)* or Wiedenmann et al. (2002) (*henceforth WI02*), or use indexes derived from dynamical properties related to blocking patterns, as the meridional potential temperature (θ) gradient on a potential vorticity (PV) surface representative of the tropopause (Pelly and Hoskins, 2003) or negative anomalies of vertically integrated potential vorticity within the 500-150 hPa layer (Schwierz et al., 2004).

As a result, several long-term studies focused on North Hemisphere blocking events have been published (Rex, 1950a, b; LO83; Dole and Gordon, 1983; TM90; Tibaldi et al., 1994; LS95; WI02). However, some of them are usually confined to certain regions or limited to single seasons. Moreover, the behavior of the North Hemisphere (NH) blocking has been traditionally described in terms of frequency, duration and favored occurrence regions, not considering other characteristics such as genesis location, intensity and size.

On the other hand, not many studies include variability, especially at interdecadal scales (e.g., Chen and Yoon, 2002). Some authors have reported that blocking occurrence may be affected by NH large-scale patterns as the North Atlantic Oscillation (NAO) (e.g., Shabbar et al., 2001). The relationship between blocking and the El Niño-Southern Oscillation (ENSO), however, has been widely discussed (e.g., Renwick and Wallace, 1996; Watson and Colucci, 2002; WI02). Nevertheless, this linkage has been derived for certain regions or single seasons and the ENSO-related variability, if any, has not been clearly established.

Thus, this research has three objectives: *i)* to design an objective automated methodology to provide a complete characterization of single blocked flows as well as a tracking algorithm to identify persistent blocking patterns, solving some previous lacks to date; *ii)* to obtain the longest record of NH blocking occurrences and parameters providing a robust long-term climatology; *iii)* to examine the low-frequency blocking variability (from interannual to interdecadal time scales) and the role played by the main NH teleconnection patterns and ENSO.

2. DATA, METHODS, AND ANALYSES

A 55-year record (1948-2002) of daily 500 hPa height geopotential fields at 0000 UTC on a 2.5º latitude by 2.5º longitude grid for the whole NH, extracted from the NCEP/NCAR reanalysis dataset, were used (Kalnay et al., 1996; Kistler et al., 2001).

2.1 Blocking Index.

Since blocking patterns are characterized by an appreciable mass difference between high and middle latitudes (e.g., Treidl et al., 1981) and anomalous easterly winds, the blocking index used here is an adapted version of the TM90 index (see Trigo et al., 2004), which is based on the original criterion proposed by LO83. According to the LO83 criterion, a blocking event can be identified when the averaged zonal index (*LO*), computed as the 500 hPa height difference between 40ºN and 60ºN, is negative over 30º in longitude and during five or more days. However, TM90 noted that cut-off lows displaced poleward could also yield negative *LO* values. In order to exclude them, they demanded an additional negative height gradient northward of 60ºN. In agreement with that, a blocking event was detected when at least three consecutive longitudes appeared as blocked during at least five days. Following the TM90 methodology, two 500 hPa height geopotential gradients (*GHGN* and *GHGS*) have been simultaneously computed for each longitude and for each day of study over the North Hemisphere in agreement with the expression [1]:

**Corresponding author address:* Anthony R. Lupo, Dept. Soil, Environmental, and Atmospheric Sciences, 302 ABNR Building, University of Missouri-Columbia, Columbia, MO 65211. E-mail: LupoA@missouri.edu.

$$GHGN = \frac{Z(\lambda,\phi_N) - Z(\lambda,\phi_0)}{\phi_N - \phi_0}$$
$$GHGS = \frac{Z(\lambda,\phi_0) - Z(\lambda,\phi_S)}{\phi_0 - \phi_S} \quad [1]$$

$$\phi_N = 77.5^o N + \Delta$$
$$\phi_0 = 60.0^o N + \Delta$$
$$\phi_S = 40.0^o N + \Delta$$
$$\Delta = -5.0^o, -2.5^o, 0.0^o, 2.5^o, 5.0^o \quad [2]$$

where $Z(\lambda,\phi)$ is the 500 hPa height geopotential at longitude λ and latitude ϕ. *GHGS* is proportional to the zonal geostrophic wind component and provides a measure of the zonal flow intensity for each longitude, while *GHGN* gradient is imposed in order to exclude non-blocked flows. This new version of the TM90 index is based on the availability of higher resolution for the NCEP/NCAR gridded data and the latitudinal frequency distribution of blocking episodes than that used by Treidl et al. (1981) (see Trigo et al., 2004). Thus, an arbitrary longitude is considered as blocked when both, *GHGN* and *GHGS*, verify the condition expressed by Eq. (3) below, for at least one of the five Δ values, and simultaneously the ϕ_0 height anomaly is positive. Thus, this procedure incorporates better spatial resolution and more blocking opportunities by allowing five Δ values instead of the three proposed by TM90.

$$GHGN < -10\, gpm/^o latitude$$
$$GHGS > 0$$
$$Z(\lambda,\phi_0) - \overline{Z(\lambda,\phi_0)} > 0 \quad [3]$$

2.2 Automated single blocking detection.

The detection of blocking events can be summed up by consulting Fig. 3 in Barriopedro et al. (2005). Since blocking anticyclones are large-scale systems, a blocking pattern can be assumed when several adjacent longitudes are simultaneously blocked. The principle of the automated blocking method is then based on the detection of contiguous blocked longitudes persisting for several days. The blocked region extension criterion in automated methodologies has ranged from 7.5º (e.g, Trigo et al., 2004) to 18.75º (TM90). After testing the blocking index, five (12.5º) or more contiguous longitudes were required to assume a blocking pattern exists, but allowing one non-blocked longitude between two blocked longitudes. This additional condition is imposed in order to include those blocking patterns showing non-blocked longitudes under an anticyclone area. Thus, in agreement with Verdecchia et al. (1996) and Tibaldi et al. (1997), three consecutive blocked longitudes can sometimes be enough for defining a blocking pattern. By applying the mentioned criteria, blocking anticyclones were initially detected and characterized by the date of occurrence, the first eastern blocked longitude (λ_0) and their extension (*S*), evaluated as the number of blocked longitudes.

2.3 Center Detection.

Unlike previous methodologies, the detection process incorporates a new procedure to detect the center of blocking. The blocking center is assumed to be the maximum height grid point within the closed or quasi-closed region of anticyclonic flow. This new parameter provides a better characterization of the blocked flow and a useful tool to track the blocking evolution.

An analysis showed that the longitude of the blocking center is not always confined within the blocked region (defined by the adjacent blocked longitudes), especially when an Ω-block occurs. Under this configuration, blocked longitudes sometimes extend slightly eastward or/and westward of the blocking center showing small negative or near zero *GHGS* values. Since the blocking center should be located in the blocked region, a longitude and latitude box centered within the blocked region was constructed. The longitude limits extend 5º east (west) of to the first (last) blocked longitude, in order to ensure that the block center is included in the box. The latitude thresholds were selected as those northward (southward) of the maximum (minimum) value of ϕ_S (ϕ_N). The method selects those grid points where the averaged height is maximum within the box. Thus, the longitude center is chosen as that longitude within the box with maximum height latitudinally averaged for box limits. Once the blocking longitude is detected, the latitudinal center is that for the selected longitude center displaying the highest longitudinal averaged height value within the box .

2.4 Blocking Intensity.

A blocking intensity index (*BI*) was also computed following a methodology similar to LS95 and WI02. This index was obtained by LS95 by normalizing the local maximum height geopotential $Z(\lambda,\phi)$ (here, the blocking center) with a mean contour line, *RC*, embracing the downstream and upstream troughs. The original index was here slightly modified as:

$$BI = 100.0 \cdot \left[\frac{Z(\lambda,\phi)}{RC} - 1.0 \right]$$
$$RC = \left[\frac{Z(\lambda_u,\phi) + Z(\lambda_d,\phi)}{2} \right] \quad [4]$$

where that mean line *RC* was obtained averaging the lowest trough axis upstream $Z(\lambda_u,\phi)$ and downstream $Z(\lambda_d,\phi)$ heights located at the same latitude of the blocking center. *BI* values are then proportional to height gradients over the blocked area and provide a measure of the large scale flow strength (LS95; WI02). The λ_u (λ_d) position was fixed 10º westward (eastward) of the half-extension from the blocking center in longitude, in order to ensure they are located in the upstream (downstream) of the blocking region.

2.5 Tracking Procedure.

Even though one of the defining characteristics of blocking events is their persistence in time, there is no commonly accepted minimum duration criterion, varying between 3 (Elliot and Smith, 1949) and 30 days (Treidl et al., 1981), although most authors tend to adopt a value of five (Treidl et al., 1981; TM90) or ten days (e.g., Rex, 1950a; Trigo et al., 2004). The designed tracking procedure incorporates both a spatial and temporal algorithms:

1) SPATIAL ALGORITHM: Although, in agreement with the Rex criterion, most simultaneous blocking occurrences showed their centers separated by more than 50º in longitude, occasionally they were found too close to be assumed as two independent blocking patterns. In these cases the duplicated blocked region showed to be only one blocking pattern. Thus, those blocking centers closer than 45º in longitude and showing blocked regions nearer than 22.5º were considered the same blocking pattern and the blocking candidate with highest height center value was selected as blocking.

2) TEMPORAL ALGORITHM: The temporal algorithm can be summarized in four steps:

   Step1: The blocked area of each blocking anticyclone in the day d_i is compared with that of each blocking in the day d_{i+1} (blocking candidates). A blocking anticyclone in the day d_i is detected the next day when at least one of its blocked longitudes continues blocked on d_{i+1}. If two or more blocking candidates meet this condition, the blocking with more common blocked longitudes is considered as the following location.

   Step2: In spite of step1, a few events with a low number of blocked longitudes did not show a blocked area overlap with any of the next days blocking longitudes. To include these situations, an event in the day d_i can be linked to a previously non-assigned d_{i+1} blocking if their blocked areas are closer than 22.5º longitude and their centers nearer than 20º longitude.

   Step3: Following the criterion proposed by Trigo et al. (2004), a non-blocked day is allowed between two blocked days for a given blocking anticyclone. That means that, if a non-assigned d_i blocking is detected on d_{i+2} day -verifying the step1 or step2 distance restrictions-, they are considered the same blocking. This is also consistent with the LS95 criterion.

   Step4: In agreement with the most widely accepted criteria, a minimum duration of 5 days is demanded to blocking events, although, according to the previous step, the blocking could be detected intermittently.

Once blocking episodes were identified, the daily parameters λ, ϕ, λ_0, S and BI were averaged for the whole life cycle of each event and in order to provide a blocking event characterization. This yields a 55-year NH data base of blocking events described by the date of initiation, duration and mean and maximum characteristic values of location (affected region), extension (size) and intensity.

3. A 55-YEAR NH CLIMATOLOGY

3.1 Temporal and Spatial Distributions.

In the 55 year period, a total of 1514 blocking events were detected over the NH, an annual average of about 27 events. About half the days per year were blocked on average over any region of the NH. Although a smaller number of events were obtained in earlier studies (e.g. Treidl et al., 1981; LO83) this result is close to those reported in the later works, as in WI02 who, using NCEP/NCAR data sets, found an annual frequency of 25 events. Blocking event durations showed an exponentially decreasing and long-tailed distribution, while the extension and intensity distributions are almost normally distributed with values in the 5-30 days, 12.5-60º and 0.5-5 ranges, and averages of 9 days, 30º and 2.5, respectively. Similar values have been found in previous climatologies (LO83; TM90; Tibaldi et al., 1994; LS95; Colucci and Alberta, 1996; WI02) although the averaged blocking intensity is slightly lower than that obtained by WI02. The seasonal distributions are also similar to those in previous studies with a higher occurrence both for blocking events and blocked days during winter and spring seasons, a frequency minimum in summer, as well as greater durations, intensities and extensions in winter than in summer.

Figure 1a displays the annually averaged frequency of blocked longitudes distribution for the whole period. As has been extensively noted in the literature, two main sectors with a higher tendency for blocking can be distinguished, encompassing Euro-Atlantic and Pacific regions respectively (Rex, 1950a, b; LO83). The Pacific blocking activity extends between 100ºE and 240ºE with a maximum located near the Central Pacific (180º) while the Euro-Atlantic counterpart is more prominent expanding from 270ºE to 90ºE with greater frequencies near 10ºE. Both bands of blocked longitudes are separated by regions of preferred zonal flow centered in 100ºE and 270ºE. The formation and maintenance of blocking events over these sectors has been dynamically attributed to the increased storm-track activity occurring downstream of the main continental areas of North America and Asia (Shutts, 1983, 1986; Colucci, 1985; Konrad and Colucci, 1988; Tsou and Smith, 1990; LS95). However, differences in the spatial distribution for the latitude of the center have been found over Euro-Atlantic and Pacific regions. Thus, although blocks tend to concentrate within the 60º-70ºN band, Euro-Atlantic blocking is more common southward of 60ºN (Fig. 1b) while the Pacific activity is enhanced poleward of the 60ºN (Fig. 1c). The Euro-Atlantic (Pacific) maximum frequency northward of the 60ºN belt is nearly half (twice) that southward of the 60ºN. Simultaneously, the preferred regions over the Pacific region concentrate near the 120ºE and 210ºE southward of the 60ºN, while the 180º meridian presents higher density poleward of the 60ºN.

a)

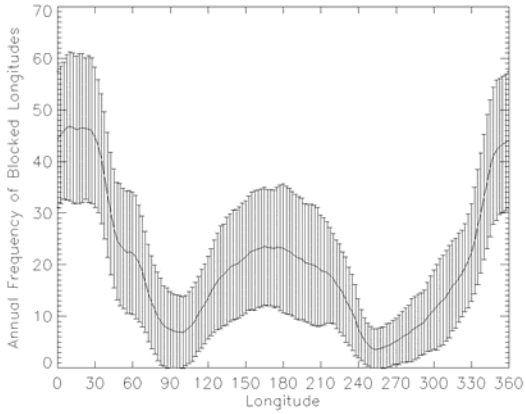

b)

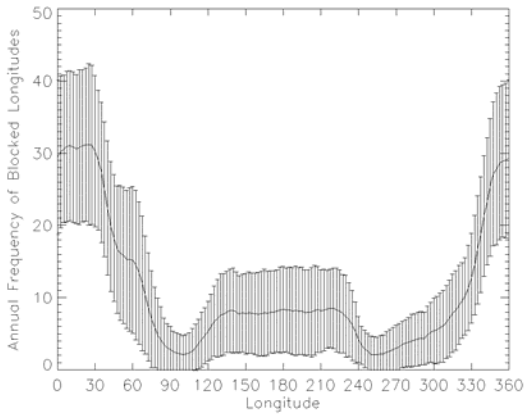

c)

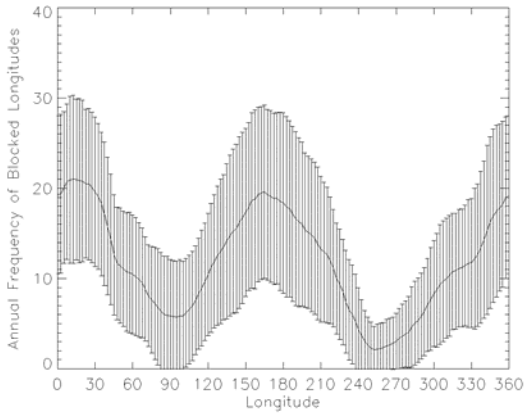

Figure 1. 55-year annually averaged frequency distribution of blocked longitudes and error bars representing the σ-deviation for: a) all events, b) events located between 50-60ºN, c) events located between 60-70ºN.

On the other hand, seasonal distributions reveal some differences in preferred blocked regions (not shown). Thus, it can be inferred that, while the Euro-Atlantic and Pacific regions present less frequent blocking activity during the summer, the blocking frequency is substantially enhanced over eastern Europe and western Asian. In some previous studies (e.g., Treidl et al., 1981; Dole and Gordon, 1983; LS95; WI02), this Euro-Asian region, usually referred as continental blocking sector, has been considered as a third preference area for blocking occurrence, independent of Euro-Atlantic and Pacific sectors, and dynamically linked to a third storm-track activity band extending along the Mediterranean Sea (e.g., Whittaker and Horn, 1981).

In order to distinguish between genesis and occurrence regions, the first-detected position and the averaged life-cycle center location of blocking events have been computed and their distributions simultaneously plotted in Fig 2. Although blocking formation zones fit well with the preferred blocked areas, confirming that blocking events are essentially quasi-stationary, the genesis density is significantly higher than the mean blocking occurrence over the east Atlantic, suggesting that blocking events originated over the Atlantic sector tend to propagate eastward towards continental regions. A similar behavior was found by Rex (1950b) and LO83. On the other hand, the eastern Pacific genesis maximum is more prominent than its western counterpart but both display similar occurrence frequencies, inferring a westward displacement of blocking events in the Pacific as well. The Euro-Atlantic (Pacific) displacement is more evident in cold (warm) seasons.

Figure 2 suggests two primary blocking episode genesis areas during the cold season: over the central Pacific and the east Atlantic oceans, near 180º and 0º, respectively. In the warm seasons the central Pacific maximum splits into two genesis bands, downstream (120ºE) and upstream (210ºE) of the Asia and North America continents respectively. Additionally, the Euro-Atlantic activity presented two genesis regions located upstream (350ºE) and downstream (30º E) of the European continent. Thus, four zones of blocking genesis can be identified for the whole NH, three of them over the oceanic-continental transition margins and one more in the Euro-Asian frontier. These distributions are also obtained by computing the 55-year blocking center seasonal distribution (not shown). In the cold season, events are relatively more frequent over Central Pacific Ocean (the Bering Strait, Aleutian Islands, Othotsk Sea, and Alaska), and over the eastern side of the North Atlantic Ocean (the British islands, the North Sea and Northwestern Europe), while the blocking activity is reduced over the continental landmasses. However, in spring and summertime, blocking centers are displaced poleward and concentrated over the ocean-continent transition margins. Fewer events are found over the Pacific and Atlantic oceans, while the blocking occurrence is substantially increased upstream and downstream of the main continental masses as well as inside Euro-Asia. These results support the existence of four different blocking sectors, suggesting a new regional division. Their domains are shown in Table 1.

Table 1. Blocking Sectors defined in this study

	Euro-Atlantic		**Pacific**	
Sector	ATL	EUR	WPA	EPA
Domain	(100ºW, 0º)	(0º, 90ºE)	(90ºE, 180º)	(180º, 100ºW)

a)

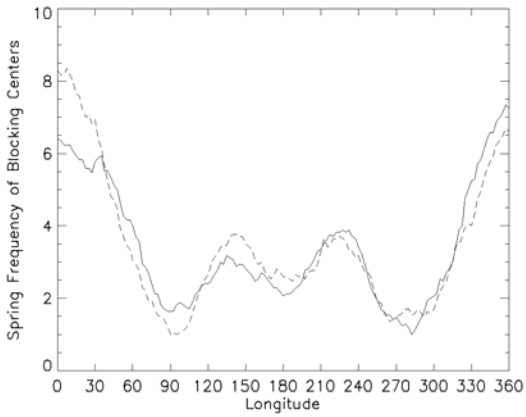

b)

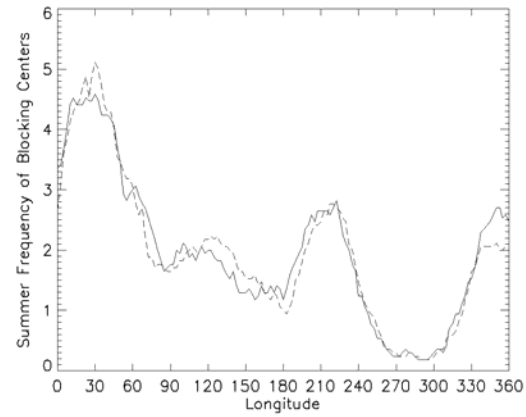

c)

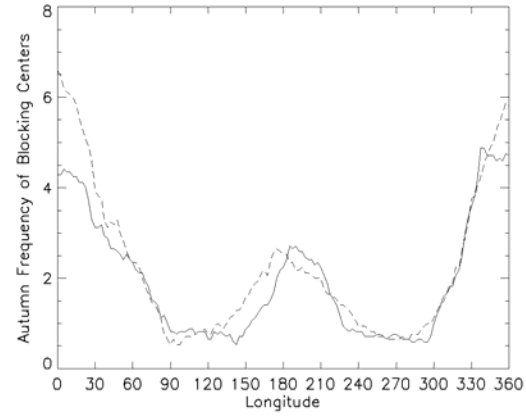

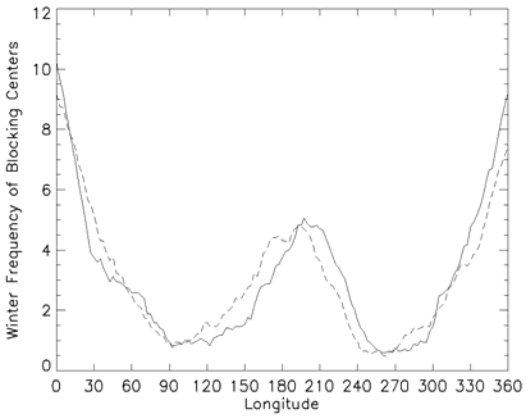

Figure 2. Seasonal longitudinal frequency distribution of genesis (solid line) and life-cycle averaged (dashed line) blocking center longitude: a) spring, b) summer, c) autumn, d) winter.

3.2 Regional blocking event characteristics.

The seasonal and regional blocking parameters are shown in Table 2. Examining the climatological averages some differences can be inferred. The seasonal frequencies reveal that blocking events are more common during the spring (winter-spring) for both EPA and WPA (ATL and EUR) as well as a minimum in blocking frequencies during the fall (summer) season. Moreover, those sectors with greater continental surface extension (EUR and WPA) show a secondary occurrence maximum in early summertime. As a result, a marked seasonal cycle is evident over the ATL and EPA sectors while in the EUR and WPA sectors, essentially confined to continental surface areas, the variability is less pronounced.

Table 2. Annual and seasonal mean (columns) of blocking parameters for the North Hemisphere and blocking sectors (rows) defined in Table1. Blocking parameters are referenced in each cell as: number of blocking events / duration (days) / BI / S (degrees).

a) Annual

	Events	Days	Intensity	Size
ATL	6.6	8.9	2.8	30.3
EUR	10.6	9.2	2.4	29.1
WPA	5.1	8.5	2.1	31.0
EPA	5.2	8.4	2.8	29.2
TOT	27.5	8.8	2.5	29.8

b) Spring

	Events	Days	Intensity	Size
ATL	2.3	8.5	2.5	29.5
EUR	3.1	9.3	2.2	28.3
WPA	1.7	8.7	1.8	29.2
EPA	1.7	8.1	2.2	27.9
TOT	27.5	8.7	2.2	28.7

c) Summer

	Events	Days	Intensity	Size
ATL	0.7	7.0	2.1	23.8
EUR	2.4	8.3	1.9	25.9
WPA	1.2	7.2	1.6	27.5
EPA	1.0	6.7	1.8	22.9
TOT	5.3	7.5	1.8	25.4

d) Fall

	Events	Days	Intensity	Size
ATL	1.7	9.4	3.0	30.8
EUR	2.4	8.9	2.8	28.8
WPA	0.8	8.0	2.6	32.8
EPA	0.9	8.1	3.2	29.4
TOT	5.8	8.8	2.9	30.1

e) Winter

	Events	Days	Intensity	Size
ATL	1.9	9.6	3.1	33.6
EUR	2.7	10.0	2.9	33.4
WPA	1.4	9.7	2.7	35.3
EPA	1.6	10.0	3.7	34.0
TOT	7.6	9.9	3.1	34.0

When examining annual averages, long-lasting episodes are essentially confined to the European sector, its difference with Pacific sectors being statistically significant at $p<0.1$ confidence level using the t-test. A seasonal breakdown showed more persistent events in the summer over those sectors with high continental presence (EUR and WPA), especially in EUR ($p<0.1$), whereas during winter, long-lived episodes occur over the oceans (ATL and EPA), although differences were not significant at the $p<0.1$ level.

Those events that occurred in the oceanic regions (ATL and EPA) presented significantly greater intensities ($p<0.05$) in all seasons. Greater block extensions were usually associated with those episodes occurring downstream of the main continents (continent-ocean margins), except in summer and winter, when they are located over continents and Pacific sectors, respectively, although seasonal extension differences were only statistically significant in summer ($p<0.1$). The annual variability of intensity and extension was characterized by stronger and greater cold season episodes in all sectors but more evident in ATL and EPA sectors.

In summary, long-lived (high-extension) events were relatively more common over the continental regions in the warm seasons and over the oceanic (Pacific) sectors in wintertime, while the strong/weak frequency ratio was higher over the oceanic sectors in all seasons. Additionally, long-lived episodes did not only tend to be more intense as reported LS95, but also tend to show greater extensions, especially for ATL and EPA sectors ($p<0.01$).

4. LONG TERM VARIABILITY

In recent years, long-term blocking variability has been associated with variability of large-scale circulation anomalies (Renwick and Wallace, 1996; Shabbar et al., 2001; WI02). However, as shown previously, there has been no complete eaxmination of the influence of teleconnections due to the limited time periods and regions used in those previous studies. In this section, the long-term trends and regional variability of blocking parameters related to teleconnection patterns (TCPs) were analyzed for the whole NH.

4.1 Series and Trends.

For every blocking parameter series global and regional trends have been examined by calculating the slope of the linear regressions versus time. Statistical significance has been assessed using a student t-test, with significance level of $p<0.1$. Table 3 displays the annual significant results computed as the relative change for the 55-year period.

Table 3. The relative annual changes (%) in each blocking parameter for the 55-year period. Significant trends at $p<0.1$, 0.05 and 0.01 are shown in italic, italic-bold and bold, respectively.

Reg	Blocking Days	Blocking events	Duration	Intensity	Size
ATL	*- 21.2*	*- 20.9*	-	*- 11.6*	***- 8.8***
EUR	*- 17.6*	-	***- 17.6***	-	-
WPA	**57.0**	**62.4**	-	-	-
EPA	-	-	-	*- 9.8*	*8.8*
TOT	-	-	*- 8.2*	*- 5.5*	-

The 55-year series in the annually averaged number of blocked days and blocking episodes did not reveal any significant long-term trend for the whole NH in agreement with WI02. Breaking down the entire NH into sectors, the EUR (ATL) sector showed a significant downward trend with a 55-year decrease of –17.6% (-21.2%) in blocked days frequency while a linear increase of 57.0% blocked days was found significant over the WPA sector for the whole period. Examining the series by season, the positive (negative) WPA (ATL) trend was confined to spring (winter), while none of the seasonal EUR series reached any significant change in blocking days.

Examining the long-term variability in the number of blocking events, the annual and spring series in the WPA events also displayed significant upward trends. There were analogous decreases in the number of annual and winter ATL events. These trends are in agreement with those obtained in the number of blocked days, whereas no significant trends were found in EUR events. As a whole, the regional trends over ATL and EUR lead to decrease blocked days (-19.6%) and events (-21.0%) in winter for the entire NH, while the upward trend in WPA sector produced a simultaneous increase in the number of spring blocking events (28.8%) but not in blocked days.

On the other hand, there was an overall NH long-term change towards less persistent and less intense blocking events. This agrees with the results of Lupo et al. (1997), which showed, using a climate model, that blocking events would be less intense and less persistent in a warmer climate,. The global trend in duration was only significant in the EUR sector at the regional level, with an annual decreasing trend of –17.6% for the 55-year period. As a consequence, while the

increased (decreased) number of blocked days in the WPA (ATL) resulted in an increase (decrease) in the number of events, the negative EUR duration trend can be associated with the simultaneous decrease in blocked days. With regard to blocking intensities, the negative annual trend was observed in ATL, EUR and EPA sectors, especially in warm seasons, although only significant over the ATL and EPA sectors. However, unlike the global behavior, WPA blocking intensities tended to increasing values (not significant).

4.2 Teleconnection patterns.

In order to explore blocking variability, the main NH variability patterns have been included in this study: North Atlantic Oscillation (NAO), East Atlantic (EA), East Atlantic Jet (EAJ), East Atlantic-Western Russia (EAWR), Scandinavian (SCAN), West Pacific (WP), East Pacific (EP) and Pacific North America (PNA) patterns (e.g., Wallace and Gutzler, 1981; Barnston and Livezey, 1987). Indexes obtained from the first rotated empirical orthogonal function (EOF) of 700-hPa fields have been extracted from the Climatic Prediction Center (CPC) at NOAA website (www.cpc.ncep.noaa.gov). In order to assess the global ENSO influence on blocking occurrence and compare with those results provided in the literature, a monthly ENSO index has also been obtained from the NOAA CPC website, which is based on a running mean Pacific Ocean basin SST anomaly over the El Niño-3 region (5°N-5°S; 150º-90°W). Monthly series have been annually and seasonally averaged with winter defined as JFM period.

Once the averaged indexes have been computed, those values departing from the climatic mean at the 0.5-sigma level (standard deviations) above (below) are considered as periods in which the pattern remained in positive (negative) phase.

The influence of the main TCPs on blocking frequency variability has been investigated for every sector at annual and seasonal scales through a multiple stepwise regression. This statistical procedure selects the independent variables to include in a multiple regression model, assuming that some inputs do not have an important explanatory effect on the response due to their multicollinearity. The basic procedures involve (1) identifying an initial model from those variables that explain a significant percentage of variability ($p<0.05$ from a t-test of regressed coefficients), (2) repeatedly altering the model at the previous step by adding (forward step) or removing (backward) a predictor variable in accordance with a specified critical output value ($p<0.1$) and (3) finishing the search when all input variables steps have been included or removed. Following this procedure, the role of TCPs was considered relevant when at least one of the independent patterns in the stepwise regression accounted for more than 20% of blocked days variability. The outstanding loading patterns for each blocking sector and each analyzed period are summarized in Table 4.

The analysis showed that, at annual scales, the TCPs did not have a significant impact on any regional blocking occurrence, with no one accounting for more than 5% of the variance. As shown below, the role of TCPs was essentially limited to cold seasons, whereas in warm seasons blocking variability was not related to the TCPs.

Table 4. The influence of TCP's in regional blocking occurrence computed as the percentage of explained variance from a multiple stepwise regression (in brackets). TCPs in italic indicate negative correlations. Only significant modes explaining more than 20% of the total variance are shown.

Reg	Spring	Summer	Fall	Winter
ATL	-	-	*NAO* (23.4%)	*NAO* (44.9%)
EUR	-	-	SCAN (20.8%)	SCAN (30.0%)
WPA	*WP* (23.9%)	-	-	-
EPA	-		-	*EP* (38.3%)

i) *Atlantic Sector.*

The NAO appeared as the leading variability pattern during autumn and winter, accounting for the 25% and 45% of the blocking frequency variance, respectively. During the negative phase of the NAO (not shown), the number of ATL winter (fall) blocking days is 31.7 (21.1), the difference being significant at $p<0.01$ ($p<0.05$) from those occurring during the positive phase of the NAO of 12.7 (9.2). The duration of blocking events was also sensitive to the NAO phase, although only significant for the winter season. Thus, when the NAO was in the negative phase, blocking events lasted more than 11 days on average, much longer than during the positive phase (8 days) ($p<0.05$). These results are in agreement with those obtained by Shabbar et al. (2001). They found 67% more winter blocking days and greater lifetimes during the negative phase of the NAO. However, as demonstrated here, there was also a strong dependence between fall blocking occurrence and the NAO. There was also a significant ($p<0.01$) northward displacement of almost 5º ($p<0.01$) during the negative phases of the NAO for both, winter and autumn, as well as a westward extension of the averaged autumn and wintertime blocking locations of about 10º ($p<0.1$).

ii) European Sector.

The multiple regression analysis showed the main SCAN influence during the winter season, with about 30% of the EUR blocking frequency explained variance. SCAN was also the dominant pattern during fall, but only accounting for 20% of the variance. Winter positive phases of the SCAN (not shown here) reveal an average annual frequency of 36.5 blocked days, which is double that occurring for the negative phases (14.6) ($p<0.01$). Also, when SCAN was in the positive phase, 30% longer blocking episodes were observed over Europe ($p<0.1$) and blocking center locations were on average 5º northward ($p<0.01$) and 5º eastward ($p<0.1$) shifted towards inner Europe.

iii) West Pacific Sector.

An examination of WPA blocking variability showed the WP pattern as the primary mode of variability during all the year, being especially prominent during spring, when it explained about 25% of the blocking frequency variance. Significant differences ($p<0.01$) between blocking frequency in the positive and negative phases of the WP were found in

spring, with values in the negative phase (16.2) being twice those of the positive phase (7.6). However, differences in block persistence were not significant. It was the phase of the WP that determined pronounced zonal variations in the location and intensity of the Asian jet stream, when WP was in the negative phase more blocks were located in the eastern portion of the WPA sector ($p<0.1$), with an averaged eastern displacement of almost 10º in longitude.

iv) East Pacific Sector.

The only relevant TCP influence on the EPA blocking frequency was limited to winter, when EP accounted for more than 35% of blocking variance. During the negative phase of EP the winter average number of blocked days in the EPA sector was 24.1, versus 8.6 days for the positive phase ($p<0.01$). Winter blocking events were also 15% longer during the negative phase of the EP, although the difference was not significant at $p<0.1$. Positive values of EP were associated with a pronounced northeastward extension of the Pacific jet and enhanced westerlies over the western North America. In contrast, during the negative phases, westerlies were reduced and the split-flow configuration over the North Pacific favored blocking occurrence. Thus, blocks were more frequent over Alaska and the Bering Strait and averaged blocking centers were (3º) south and (8º) westward displaced ($p<0.1$) when EP was in the negative phase.

v) ENSO-related variability.

The ENSO cycle exhibits a strong influence on blocking intensities and durations, especially in winter and over the EPA and WPA sectors, with longer and more intense blocking events when La Niña (LN) is dominant. The averaged winter blocking intensity during LN phase was 3.2 for the whole North Hemisphere, whereas when the ENSO was in the warm phase, the winter mean was 2.7, the difference being significant at $p<0.01$. By sectors, winter ATL, EUR, WPA and EPA blocks were 14% ($p<0.05$), 15% ($p<0.05$), 16% ($p<0.05$) and 52% ($p<0.01$) stronger during LN, respectively, in agreement with those results reported by WI02. Also, blocking events were 23% (42%) longer over the WPA (EPA) sector for LN ($p<0.05$). These results were consistent with those reported by Renwick and Wallace (1996). They found smaller 500-hPa variances during El Niño (EN) years implying more zonal flow and enhanced westerlies over the North Pacific. Since BI is proportional to meridional height gradients, it implies higher intensities occurring during LN phases (WI02).

5. DISCUSSION

5.1 The ENSO influence on blocking.

The cold phase of the ENSO has been often associated with an increase of blocking occurrence, especially over the Pacific sector and the Bering Strait in winter (Renwick and Wallace, 1996) where higher frequencies have been found during La Niña phase (LN). WI02 also found relatively more blocked days during LN phases, especially over the Pacific Sector, although differences on blocking occurrence were not significant. However, our analysis did not reveal significant differences related to the ENSO in the frequency of EPA or WPA blocked days. These discrepancies may be attributed to the higher regional resolution of blocking sectors considered here. Another explanation could be related with the ENSO influence in determining preferred blocking formation locations, but not blocking occurrences. A t-test on blocking frequency revealed more westward blocked days during the cool phase of the ENSO relative to those occurring during EN phases over the Pacific. Thus, when the ENSO in is the LN phase, blocking occurrence is westward displaced and fewer blocks occur over the EPA sector. Simultaneously, a similar increase of blocking frequencies was found in WPA sector without any significant frequency change over the whole Pacific. In fact, WPA blocked days increase during LN phase, while EPA sector presents more blocked days during EN years, although these results were not significant at $p<0.1$. Additionally, blocking center locations were displaced 10º westward ($p<0.05$) when ENSO was in LN phase. Thus, the ENSO signal over the Pacific sector seems limited to determining favored regions susceptible of blocking formation, but not to blocking frequencies, reflecting the non-linear ENSO nature, consistent with LN patterns showing a non-opposite response to that of the EN. These results are in agreement with Mullen (1989) who, analyzing GCM simulations, found that the ENSO and SST anomalies do not affect blocking frequency but the preferred locations for block formation over the Pacific region.

5.2 The dynamic role of TCP's in blocking occurrence.

Several theories have been proposed on formation and maintenance of blocking events. Some of them are based on non-linear interactions either between planetary waves (e.g., Egger, 1978; Kung et al., 1990) or between large-scale flow and transient eddies (Reinhold and Pierrehumbert, 1982). Others are related to amplified Rossby waves due to barotropic (e.g., Simmons et al., 1983) or baroclinic (e.g., Frederiksen, 1982) instability. A number of them defend that blocks may be the result of the adjustment of the planetary waves to deviations in the zonal mean flow (e.g., Kaas and Branstator, 1993), or the linear resonance of planetary waves with the surface forcing (e.g, Tung and Lindzen, 1979). Additionally, conceptual models link low-frequency transient eddies and blocking events (e.g, Shutts, 1983; Tsou and Smith, 1990). Recently, Shabbar et al. (2001) demonstrate the decisive contribution of the NAO to the wintertime blocking occurrence over the Atlantic sector, establishing a simple conceptual model based on the Charney and DeVore (1979) theory. According to this theory, blocking phenomenon is a metastable equilibrium state between two equilibrium solutions of high-index flow (weak wave-like component) and low-index flow (strong wave component). They also state that the stability of the (blocked) flow can be discussed in a regional context. This view is consistent with the findings of Lupo (1997), and Lupo et al. (2005), in that they find blocking events persist as long as the planetary-scale flow is quasi-stable. Shabbar et al. (2001) offer a dynamical explanation relating the NAO, blocks and the zonally asymmetric thermal forcing as induced by the land-sea temperature contrast. The phase of the NAO determines the land-sea zonal temperature distribution, favoring or inhibiting the resonance interaction phase between topographic and

thermal forcing, and, hence, the greater or lower occurrence of blocks.

Following this model, the surface air temperature (SAT) composites have been computed for both polarities of the significant TCP from the monthly surface air temperature fields of the NCEP/NCAR reanalysis, and their differences examined through a t-test ($p<0.05$). The composite difference of SAT between the positive and negative phases of the NAO, SCAN, WP and EP patterns in winter, when the TCP influence on blocking frequency is relevant were tested here (not shown). The associated patterns reflect a temperature dipole of opposite sign over land and ocean, such that, when the pattern is in the phase favoring the blocking occurrence, a general contrast "warm ocean/cold land" pattern is dominant. For the ATL sector and a negative phase of the NAO, the warming is located over the Baffin Bay and Labrador Sea, while a general cooling occurs over the north Europe and Asia continents. On the other hand, when the SCAN is in the positive polarity, a pronounced cooling affects inland Europe accompanied by a relative warming over the North Sea and Greenland. The positive EP pattern reflects a thermal dipole with positive anomalies inland North America and negative over the Bering Strait. Thus, winter blocking variability is coherent with the conceptual model proposed by Charney and DeVore (1979) and Shabbar et al. (2001), linking blocking occurrence and dynamical TCP forcings in ATL, EUR and EPA sectors. According to the conceptual model, over these sectors the zonally asymmetric thermal and topography forcing are in phase when the "warm ocean/cold land" pattern occurs, in the sense that the thermal forcing is coupled with the topography producing a favorable environment for the formation and persistence of blocking (Shabbar et al., 2001).

Additionally, the winter WP signature is characterized by above-normal temperatures over the eastern coast of Asia and a simultaneous below-normal SATs spanning the North America continent during the negative phase of WP. In agreement with the conceptual model, the zonally asymmetric thermal forcing should favor winter WPA blocking occurrences during the negative phases of WP. However, only 14% of WPA blocking frequency variance was accounted for the WP in winter in the stepwise regression.

In order to get an explanation of these different patterns pairs of oceanic-continental regions have been selected. They are defined 20º in latitude and 40º in longitude based on those areas of maximum positive and negative SAT responses. For each TCP and blocking sector, a seasonal temperature index is defined as the box-averaged SAT differences between those boxes located over the respective oceanic and land regions:

$$\Delta(SAT)_S = \left(\overline{SAT}_S^{Oc} - \overline{SAT}_S^{Co}\right) \quad [5]$$

where the subindex S represents the sector and the superindex Oc (Co) indicates the oceanic (continental) box. This index provides a measure of the average zonal air temperature difference between oceanic and continental regions. When linear correlations are computed between blocking days and winter Δ(SAT) indices the magnitude of the link reaches 0.68, 0.51 and 0.53 ($p<0.01$) for ATL, EUR and EPA, respectively. These results confirm that the associated TCPs (NAO, SCAN and EP, respectively) exert a potential control in blocking atmospheric circulation by inducing anomalous longitudinal gradients of surface temperature. These land-sea contrasts may influence blocking occurrence through the temperature-associated formation of anomalous zonal wind gradients. However, the correlation coefficient falls to 0.24 (not significant) for WPA sector, suggesting a characteristic blocking behavior over the WPA sector. This is consistent with the findings of Nakamura et al. (1997) and Lupo (1997) who examined the relative contributions of large and synoptic-scale processes in Pacific and Atlantic region blocking events. The long-term trend analysis provided in the last section also supports this assertion, with long-term WPA series presenting a significant trend in blocking frequency, opposite in sign to the other regional trends. This distinctive behavior suggests that additional mechanisms may control the asymmetrical temperature distribution over Eurasian sector more than WP pattern. The dynamical link could be attributed to the unique surface conditions associated with thermal (Eurasian snow cover) and/or topography (Himalayas) forcing mechanisms operating over Asia continent. Anomalous North Pacific SST could act as a potential contributor to WPA blocking variability.

5.2 Changes in atmospheric blocking.

The long-term analysis in blocking frequencies has shown a downward (upward) trend in blocking days over ATL and EUR (WPA) sectors. The observed changes over ATL and WPA are in concert with simultaneous changes in blocking occurrence, while the EUR trend is more related to significant decreases in blocking durations than in the number of blocking events. These results suggest that those observational trends could be partially explained by simultaneous changes in the forcing factors responsible of blocking formation (ATL and WPA) and maintenance (EUR), respectively.

In the context of the conceptual model discussed in the last section, regional modes have shown to modulate blocking occurrence through the anomalous TCP-associated temperature distributions. Thus, recent trends in surface temperature could be partially responsible of the observed trends in blocking occurrence.

Hurrell (1996) and Thompson et al. (2000) evaluated the contribution of the NAO/AO to recent wintertime surface air temperature trends, with the NAO accounting for about 30% of the hemispheric interannual variance and about half of the cooling in the northwest of North America and the warming over Europe. Thus, the strong association between the NAO and blocking occurrence points the recent upward NAO trend as a potential contributor to the observed decreasing trends in the ATL sector.

However, since the WP mode only accounts for a low percentage of WPA blocking occurrence, this pattern cannot explain the upward trend in WPA blocking occurrence. Indeed, the recent positive trend in WP index is opposite to that expected accordingly to the increase of WPA blocking occurrence and the negative relationship between them.

On the other hand, the observed decreases in blocking days and durations over the EUR sector would be expected to result from significant changes in those mechanisms controlling blocking persistence. Several studies have shown

the decisive contribution of surface synoptic disturbances and explosive cyclogenesis westward-block located in the maintenance of blocking events (Shutts, 1983, 1986; Colucci, 1985; Konrad and Colucci, 1988; Tsou and Smith, 1990; LS95). Simultaneously, relevant changes in North-Atlantic storm-track activity that affect the western European sector have been found in winter (March), with significant decreases in cyclone densities near the Iberian Peninsula (Paredes et al., 2005).

However, further investigations on the sustaining mechanisms of blocking as well as on the forcing factors of WPA blocking are required to provide more evidence of the observed trends over these sectors.

6. SUMMARY AND CONCLUSIONS

In this paper, an automated algorithm method to detect blocking single structures and events has been developed, based on a modified version of the TM90 zonal index. The new methodology excludes those synoptic structures that do not reflect a typical blocking pattern and includes those blocks detected intermittently with some longitudes within the blocked anticyclone appearing as non-blocked. Additionally, some new parameters, as blocking center locations, size and intensity have been derived for a better characterization of blocked flow. The new methodology also includes a tracking algorithm. It allows a comprehensible assimilation and definition of blocking events and durations following the individual evolution of single blocked flows. Some problems derived from the traditional methods when identifying persistent blocking (episodes) that could reflect different blocked flows are thus avoided.

The application of this objective algorithm has allowed the compilation of the longest blocking climatology for the Northern Hemisphere to date. This study provides robust results in a statistical sense, describing 55 years of blocking occurrences and parameters.

A new classification of blocking activity sectors has been proposed, providing a finer picture of regional blocking behavior. Four sectors (ATL, EUR, WPA and EPA) have been defined according to different seasonal blocking distributions. The regional characterization shows that long-lasting events and greater extensions and intensities were more common in the oceanic sectors, especially in cold seasons, while blocking events were relatively more frequent in continental sectors in warm seasons.

This study shows that TCPs play a limited role on blocking occurrence. No TCP-related blocking variability has been found for the entire year, with the signal essentially confined to the winter season. In winter just one pattern appeared as the leading variability mode of blocking frequency over each region, all of them explaining more than 20% of variance, except in the WPA sector. Only the WPA sector revealed a significant signal in spring.

It has been found that regional blocking variability mostly reacts to their regional TCP counterparts, especially for frequency and duration parameters, supporting the blocking regional classification proposed in this paper. Thus, the primary TCP modulating blocking occurrences over ATL, EUR, WPA and EPA sectors were respectively NAO, SCAN, WP and EP, although some slightly different season-related dependences have been found in WPA sector. Unlike the rest of the sectors, WPA did not show a leading mode in winter but in spring. Additionally, this study has shown that the ENSO influence was restricted to blocking intensities, with more intense blocking events occurring during LN phase, especially over the EPA sector. On the other hand, no ENSO signals have been found in blocking sector frequency.

The link between TCPs and winter blocking occurrence has been attributed to the TCP-associated formation of anomalous longitudinal gradients in surface air temperature, identifying the surface forcing and the thermal land-sea contrast as potential contributor to blocking occurrence variability in interannual and interdecadal scales. However, WPA variability was not coherent with the conceptual model proposed by Charney and DeVore (1979), suggesting that dynamical blocking mechanisms operating in the WPA may be different from those in the other sectors

7. ACKNOWLEDGMENTS

The Spanish Science and Technology Department supported this study trough the VALIMOD (Climatic VALIdation of Conceptual MODels) project (REN2002-04558-C04-01).

8. REFERENCES

Barriopedro, D., R. Garcia-Herrera, A.R. Lupo, and E. Hernandez, 2005: A climatology of Northern Hemisphere blocking. *Under review, J. Climate.*

Barnston, A. G., and R.E. Livezey, 1987: Classification, seasonality and persistence of low-frequency atmospheric circulation patterns. *Mon. Wea. Rev.*, **115**, 1083-1126.

Charney, J.G. and J.G. DeVore, 1979: Multiple flow equilibria in the atmosphere and Blocking. *J. Atmos. Sci.*, **36**, 1205-1216.

Chen, T.C., and J.H. Yoon, 2002: Interdecadal Variation of the North Pacific Wintertime Blocking. *Mon. Wea. Rev.*, **130,** 3136 – 3143.

Colucci, S.J., 1985: Explosive cyclogenesis and large-scale circulation changes: Implications for atmospheric blocking. *J. Atmos. Sci.*, **42**, 2701-2717.

_____, and T.L. Alberta, T.L., 1996: Planetary-scale climatology of explosive cyclogenisis and blocking. *Mon. Wea.. Rev.*, **124**, 2509-2520.

Dole R.M. and N.D. Gordon, 1983: Persistent anomalies of the extra-tropical northern hemisphere wintertime circulation: geographical distribution and regional persistence characteristics. *Mon. Wea. Rev.*, **111**, 1567-1586.

Egger, J. 1978: Dynamics of blocking highs. *J. Atmos. Sci.*, **35**, 1788-1801

Elliot, R.D. and T.B. Smith, 1949: A study of the effect of large blocking highs on the general circulation in the northern hemisphere westerlies. *J. Met.*, **6**, 67-85.

Frederiksen, J.S., 1982: A unified three-dimensional instability theory of the onset of blocking and cyclogenisis. *J. Atmos. Sci.*, **39**, 969-987.

Hurrell, J.W., 1996: Influence of variations in extratropical wintertime teleconnections on Northern Hemisphere temperature. *Geophys. Res. Lett.*, **23**, 665-668.

Kaas, E. and G. Branstator, 1993: The relationship between a zonal index and blocking activity. *J. Atmos. Sci.*, **50**, 3061-3077.

Kalnay E., M. and co-authors, 1996: The NCEP/NCAR 40-year reanalyses project. *Bull. Am. Meteorol. Soc.*, **77**, 437-471.

Kistler, R., E. and co-authors, 2001: The NCEP–NCAR 50–Year Reanalysis: Monthly Means CD–ROM and Documentation. *Bull. Am. Meteorol. Soc.*, **82**, 247–268.

Konrad, C.E. and S.J. Colucci, S.J., 1988: Synoptic climatology of 500 mb circulation changes during explosive cyclogenesis. *Mon. Wea. Rev.*, **116**, 1431-1443.

Kung, E.C., C.C. DaCamara, W.E. Baker, J. Susskind, and C.K. Park, 1990: Simulations of Winter Blocking Episodes using Observed Sea Surface Temperatures. *Quart. J. Roy. Met. Soc.*, **116**, 1053-1070

Lejenäs, H. and H. Øakland, 1983: Characteristics of northern hemisphere blocking as determined from long time series of observational data. *Tellus*, **35A**, 350-362.

Liu, Q., 1994: On the definition and persistence of blocking. *Tellus*, **46A**, 286-290.

Lupo, A.R. and P.J. Smith, P.J. 1995: Climatological features of blocking anticyclones in the Northern Hemisphere. *Tellus*, **47A**, 439-456.

____, 1997: A diagnosis of two blocking events that occurred simultaneously over the mid-latitude Northern Hemisphere. *Mon. Wea. Rev.*, **125**, 1801 – 1823.

____, R.J. Oglesby, and I.I. Mokhov, 1997: Climatological features of blocking anticyclones: A study of Northern Hemisphere CCM1 model blocking events in present-day and double CO_2 concentration atmospheres. *Clim. Dynam.*, **13**, 181 – 195.

____, A.R. Kunz, I.I. Mokhov, and S. Dostoglou, 2005: The impact of the planetary scale on the decay of blocking and the use of phase diagrams in examining the problem. *Proceedings of the 21st Conference on Weather Analysis and Forecasting, Washington DC,* 1 – 4, August 2005.

Mullen, S. L., 1989: Model Experiments on the Impact of Pacific Sea Surface Temperature Anomalies on Blocking Frequency. *J. Climate*, **2**, 997–1013.

Nakamura, H., M. Nakamura, and J.L. Anderson, 1997: The role of high and low frequency dynamics and blocking formation. *Mon. Wea. Rev.*, **125**, 2074 - 2093.

Paredes, D., R.M. Trigo, R. García-Herrera and I.F. Trigo, 2005: Understanding precipitation changes in Iberia in early spring: weather typing and storm-tracking approaches. *J. Hydrometeor., in press*.

Pelly, J. and B. Hoskins, 2003: A new perspective on blocking, *J. Atmos. Sci.*, **60**, 743– 755.

Reinhold, B. B. and R.T. Pierrehumbert, 1982: Dynamics of Weather Regimes: Quasi-Stationary Waves and Blocking. *Mon. Wea. Rev.,* **110**, 1105–1145

Renwick, J.A. and J. M. Wallace, 1996: Relationships between North Pacific wintertime blocking, El Nino, and the PNA pattern. *Mon. Wea. Rev.*, **124**, 2071–2076.

Rex, D.F., 1950a: Blocking action in the middle troposphere and its effect upon regional climate. Part I.: An aerological study of blocking action. *Tellus*, **2**, 196-211.

___, 1950b: Blocking action in the middle troposphere and its effect upon regional climate. Part II: The climatology of blocking action. *Tellus*, **2**, 275-301.

Schwierz, C., M. Croci-Maspoli, and H.C. Davies, 2004: Perspicacious indicators of atmospheric blocking. *Geophys. Res. Lett.*, **31**, 6125-6128.

Shabbar, A., J. Huang, and K. Higuchi, 2001: The relationship between the wintertime North Atlantic Oscillation and blocking episodes in the North Atlantic. *Int. J. Climatol.*, **21**, 355–369.

Shutts, G.J., 1983: The propagation of eddies in diffluent jet streams: Eddy forcing of "blocking" flow fields. *Quart. J. Roy. Met. Soc.*, **109**, 737-762.

_____, G.J., 1986: A case study of eddy forcing during an Atlantic blocking episode. *Advances in Geophysics*, **29,** Academic Press, New-York, 135-162.

Simmons, A.J., J.M. Wallace, and G.W. Branstator, 1983: Barotropic wave propagation and instability, and atmospheric telleconnection patterns. *J. Atmos. Sci.*, **40**, 1363-1391

Tibaldi, S. and F. Molteni, 1990: On the operational predictability of blocking. *Tellus*, **42A**, 343-365.

_____, S., E. Tosi, A. Navarra, and L. Pedulli, 1994: Northern and Southern hemisphere seasonal variability of blocking frequency and predictability. *Mon. Weather. Rev.*, **122**, 1971-2003.

_____, S., F. D'Andrea, E. Tosi, E. Roeckner, 1997: Climatology of Northern Hemisphere blocking in the ECHAM model. *Clim. Dyn.*, **13**, 649-666.

Thompson, D.W.J., J.M. Wallace and G.C. Hegerl, 2000: Annular Modes in the Extratropical Circulation. Part II:

Trends. *J. Climate,* **13**, 1018–1036.

Treidl, R.A., E.C. Birch, and P. Sajecki, 1981: Blocking action in the Northern Hemisphere: A climatological study. *Atmosphere-Ocean*, **19**, 1-23.

Trigo, R.M., I.F. Trigo, C.C. DaCamara, and T.J. Osborn, 2004: Winter blocking episodes in the European-Atlantic sector: climate impacts and associated physical mechanisms in the Reanalysis. *Clim. Dyn.*, **23**, 17-28.

Tsou, C.H. and P.J. Smith, 1990: The role of synoptic/ planetary-scale interactions during the development of a blocking anticyclone. *Tellus*, **42A**, 174-193.

Tung, K.K. and R.S. Lindzen, 1979: A theory of stationary long waves. 1 A simple theory of blocking. 2. Ressonant Rossby waves in the presence of realistic vertical shears. *Mon. Wea. Rev.*,**107**, 735-750.

Verdecchia, M., G. Visconti, F. D'Andrea, and S. Tibaldi, 1996: A neural network approach for blocking recognition. *Geophys. Res. Lett.*, **23**, 2081-2084.

Wallace, J. M., and D.S. Gutzler, 1981: Teleconnections in the geopotential height field during the Northern Hemisphere winter. *Mon. Wea. Rev.*, **109**, 784-812.

Watson, J.S. and S.J. Colucci, 2002: Evaluation of Ensemble Predictions of Blocking in the NCEP Global Spectral Model. *Mon. Wea. Rev.*, **130**, 3008–3021.

White, W.B. and N.E. Clark, 1975: On the development of blocking ridge activity over the central North Pacific. *J. Atmos. Sci.*, **32**, 489-502.

Whittaker, L.M. and L.H. Horn, 1981: Geographical and Seasonal Distribution of North American Cyclogenesis, 1958–1977. *Mon. Wea. Rev.*, **109**, 2312–2322.

Wiedenmann, J.M., A.R. Lupo, I.I. Mokhov, and E.A. Tikhonova, 2002: The Climatology of Blocking Anticyclones for the Northern and Southern Hemispheres: Block Intensity as a Diagnostic, *J. Climate*, **15**, 3459-3473.